

Improved modelling of liquid GeSe₂: the impact of the exchange-correlation functional

Matthieu Micoulaut⁽¹⁾, Rodolphe Vuillemier⁽¹⁾, and Carlo Massobrio⁽²⁾

⁽¹⁾Laboratoire de Physique Théorique de la Matière Condense, Université Pierre et Marie Curie, Boite 121, 4, Place Jussieu, 75252 Paris Cedex 05, France and

⁽²⁾Institut de Physique et de Chimie des Matériaux de Strasbourg, 23 rue du Loess, BP43, F-67034 Strasbourg Cedex 2, France

(Dated: June 6, 2018)

The structural properties of liquid GeSe₂ are studied by using first-principles molecular dynamics in conjunction with the Becke, Lee, Yang and Parr (BLYP) generalized gradient approximation for the exchange and correlation energy. The results on partial pair correlation functions, coordination numbers, bond angle distributions and partial structure factors are compared with available experimental data and with previous first-principle molecular dynamics results obtained within the Perdew and Wang (PW) generalized gradient approximation for the exchange and correlation energy. We found that the BLYP approach substantially improves upon the PW one in the case of the short-range properties. In particular, the Ge–Ge pair correlation function takes a more structured profile that includes a marked first peak due to homopolar bonds, a first maximum exhibiting a clear shoulder and a deep minimum, all these features being absent in the previous PW results. Overall, the amount of tetrahedral order is significantly increased, in spite of a larger number of Ge–Ge homopolar connections. Due to the smaller number of mis coordinations, diffusion coefficients obtained by the present BLYP calculation are smaller by at least one order of magnitude than in the PW case.

PACS numbers: 61.25.Em, 61.20.Ja, 71.15.Pd

Keywords:

I. INTRODUCTION

Disordered Ge_nSe_{1-n} materials feature a large variety of bonding behaviors as a function of the composition.^{1,2,3,4,5} In the liquid state, a delicate interplay between the covalent and the ionic characters sets in for increasing values of n . At $n=0.33$, this results in a network system (GeSe₂) made of predominant GeSe₄ tetrahedra coexisting with homopolar bonds and defective Ge–Se coordinations.⁶ The existence of chemical disorder in an otherwise prevailing tetrahedral network has been firmly established through the measurement of the full set of partial structure factors and pair distribution functions of liquid GeSe₂ (l -GeSe₂ hereafter).⁷ Early molecular dynamics models based on interatomic potentials were unable to predict mis coordinations and homopolar bonds.⁸ Very recently, a refined model potential for disordered GeSe₂ was made available.^{9,10} This potential reproduces qualitatively the experimental data on glassy GeSe₂, including the presence of Se–Se homopolar bonds. However, Ge–Ge homopolar bonds were absent within this description. This proves that the explicit account of the electronic structure in the expression of the interatomic forces is crucial to describe properly disordered GeSe₂ networks. Along these lines, two approaches based on density functional theory (DFT) have been employed to study l -GeSe₂ via molecular dynamics. D. Drabold and coworkers have adopted a DFT framework based on a nonself-consistent electronic structure scheme, the local density approximation of DFT and a minimal basis set.^{11,12} As an alternative, the fully self-consistent evolution of the electronic structure described within DFT (i.e. first-principles molec-

ular dynamics, FPMD in what follows) has been pursued in the case of l -GeSe₂ with the use of plane waves and pseudopotentials.^{13,14,15} A comparison of the structural properties obtained within these two approaches is provided in a recent paper for the case of amorphous GeSe₂.¹⁶

Turning our attention to the FPMD approach and to the case of l -GeSe₂, it is worth recalling the indications collected through the use of the local density approximation (LDA) within DFT. This had the effect of producing an atomic structure affected by an excessive amount of chemical disorder and homopolar bonds.¹⁴ The absence of the FSDP (first sharp diffraction peak) in the total neutron structure factor could be correlated to the lack of a predominant structural unit (the GeSe₄ tetrahedron), with comparable percentages of Ge atoms two-fold, three-fold, four-fold and five-fold coordinated.¹⁴ Interestingly, interatomic potentials featuring formal charges on the Ge and the Se atoms (+4 and -2, respectively) are able to provide a GeSe₂ network based on undefective GeSe₄ tetrahedra, together with a FSDP in the total neutron structure factor.⁸ In the search of a DFT scheme able to recover a network structure featuring the predominant presence of GeSe₄ tetrahedra, the generalized gradient approximation (GGA) for the exchange and correlation energy proposed by Perdew and Wang (PW hereafter) was adopted.¹⁷ This choice yields a very good agreement with experiments for the total neutron structure factor over the entire range of momentum transfer.¹⁴ The improvements brought about by the GGA in the PW form were found to be due to a better account of the ionic character of bonding, as shown in Ref. 14 through an analysis of the contour plots for the

valence charge densities. The larger ionicity of bonding introduced by the PW approach manifests itself through a larger depletion of the valence charge at the Ge sites and a larger accumulation around the Se atoms, the covalency remaining essentially equivalent in the LDA and in the PW scheme.¹⁴

Despite this success, detailed comparison of the partial correlations revealed the existence of residual differences between theory and experiment. The most important of these differences concerns the first sharp diffraction peak in the concentration-concentration structure factor that appears in the experiment but it is absent in our level of theory.¹⁵ In Ref. 15 these shortcomings were attributed to an insufficiently accurate description of Ge–Ge correlations. This was confirmed by the shape of the calculated Ge–Ge correlation function, much less structured than its experimental counterpart and by the excessively long (15 % more than the experimental value) first-neighbors Ge–Ge distances. Longer interatomic Ge–Ge distances and less structured Ge–Ge pair correlation functions were correlated to an overestimate of the metallic character in liquid GeSe₂. This observation can be taken as a guideline for the choice of alternative GGA recipes capable of further improving the performances of DFT and, in particular, the distribution of the valence charge densities along the bonds. In what follows, we are interested in GGA functionals enhancing a *localized* distribution of the valence electrons at the expenses of a *delocalized* one, intrinsic in schemes inspired by the uniform electron gas model, as the PW one.

With this purpose in mind, we present a new set of structural data for short and intermediate range properties in *l*-GeSe₂, based on the GGA scheme after Becke (B) for the exchange energy) and Lee, Yang and Parr (LYP) for the correlation energy.^{18,19} This recipe makes no assumption on the uniform electron gas character of the correlation energy. Therefore, it is a good candidate to correct part of the drawbacks of the PW scheme, as those arising from an overestimate of the metallic character of bonding. The comparative analysis carried out with available PW data reveals that short-range properties and the diffusion behavior compare significantly better with experiments within the the BLYP approach. The improvement is less significant for the intermediate range properties.

This paper is organized as follows. In Sec. II, we describe our theoretical model. Our results are collected in two sections, devoted to real space properties (Sec. III) and reciprocal space properties (Sec. IV). A summary of general considerations on the modelling of disordered network-forming material can be found in Sec. V. Conclusive remarks are collected in in Sec. VI.

II. THEORETICAL MODEL

Our simulations were performed at constant volume on a system consisting of 120 atoms (40 Ge and 80 Se).

We used a periodically repeated cubic cell of size 15.7 Å, corresponding to the experimental density of the liquid at T=1050 K. We refer to our previous results on *l*-GeSe₂ for an extended rationale on the choice of our system size.^{15,22} The electronic structure was described within density functional theory (DFT) and evolved self-consistently during the motion.²³

In a series of previous papers, we had adopted the PW scheme due to Perdew and Wang as a generalized gradient approximation.^{13,14,15,16,22,35,36} This amounts to go beyond the local density approximation (LDA) by using an analytic representation of the correlation energy $\varepsilon_c(\rho)$ for a uniform electron gas. This representation allows for variations of $\varepsilon_c(\rho)$ as a function of ρ and the spin polarization.¹⁷ As mentioned in the Introduction, the use of the PW scheme improves substantially upon LDA the description of both short and intermediated range order in *l*-GeSe₂. However, residual deficiencies are found within the PW when focusing on the Ge–Ge correlations, in particular at the level of the Ge–Ge interatomic distance and pair correlation function, These signatures point out an overestimate of the metallic character of bonding, implying that the ionicity at the very origin of the formation of the tetrahedral GeSe₄ coordination is undermined by an unphysical accumulation of valence electron along the bonds.

In the search of a GGA recipe correcting these defects, we resort in this work to the generalized gradient approximation after Becke (B) for the exchange energy and Lee, Yang and Parr (LYP) for the correlation energy.^{18,19} It has to be reminded that the record of reliability of the BLYP approach has been firmly assessed, as shown in a detailed comparative study of the performances of a large variety of density functional methods.²⁰ In Ref. 20, it was concluded that the BLYP method is the DFT method with the best overall performances for properties encompassing equilibrium geometries, vibrational frequencies and atomization energies of nanostructured systems. Furthermore, our choice is motivated by the consideration that no explicit reference to the uniform electron gas is made in the derivation of the LYP correlation energy. In the original LYP derivation, a correlation energy formula due to Colle and Salvetti is recast in terms of the electron density and of a suitable Hartree-Fock density matrix, providing a correlation energy and a correlation potential.^{19,21} This scheme is expected to enhance the localized behavior of the electron density at the expenses of the electronic delocalization effects that favor the metallic character. These effects are built in GGA recipes having the uniform electron gas as reference system, as the PW one. For this rationale to be generally applicable, it would be desirable to understand which systems and bonding situations are likely to be better described by BLYP than by PW. By focusing on multicomponent systems A_nB_(1-n) of concentrations *n*, the BLYP scheme is expected to be more suited than the PW one to treat bonding situations characterized by a moderate difference of electronegativity (termed Δ_{el}

hereafter) among the system components. This is especially true for compositions close to the stoichiometry, to be intended in this context as the composition at which optimal coordination between the species A and B occurs (for instance GeSe_2 within the $\text{Ge}_n\text{Se}_{(1-n)}$ family). In the case of a large Δ_{el} , the ionic contribution to bonding is sufficiently large to ensure effective charge transfer in a way essentially independent on the details of the exchange-correlation functional. This is the case of disordered SiO_2 ($\Delta_{el}=1.54$), well described as a corner-sharing network within LDA.²⁴ On lowering Δ_{el} , the amount of the valence charge density along the bonds becomes non-negligible and the relative weight of the ionic and covalent character more delicate to quantify. The case of $l\text{-GeSe}_2$ is a prototype of this situation, being characterized by $\Delta_{el}=0.54$. By choosing BLYP to improve upon PW (and LDA) one attempts to minimize electronic delocalization effects that are undesirable in any bonding situation characterized by competing ionic and covalent contributions. These ideas withstanding, we stress that the use of a GGA recipe localizing the valence electron density on the atomic sites cannot be legitimated by the simple consideration of the Δ_{el} value. Indeed, it depends also crucially on the variation of bonding with thermodynamic parameters as pressure and temperature. For instance, in the case of $l\text{-GeSe}_2$ at high temperatures, the delocalized character of bonding grows at the expenses of the localized one (due to gap closing effects), thereby making much less crucial the use of any functional localizing the electronic valence on the atomic sites.⁵

In our work, valence electrons were treated explicitly, in conjunction with normconserving pseudopotentials of the Trouiller-Martins type to account for core-valence interactions.²⁵ The wave functions were expanded at the Γ point of the supercell on a plane wave basis set defined by an energy cutoff of 20 Ry. We found bond lengths ($d_0 = 3.99$ bohr) and vibrational frequencies ($\omega = 398$ cm^{-1}), reproducing the experimental data²⁶ and the corresponding PW results quoted in Ref. 15 to within at most 2 % and 4 %, respectively.

One configuration extracted from the fully equilibrated trajectories obtained in Refs. 15 for liquid GeSe_2 with $E_c = 20$ was taken as initial set of coordinates for the present, new set of calculations carried out within the BLYP scheme. We used a fictitious electron mass of 600 a.u. (i.e. in units of $m_e a_0^2$, where m_e is the electronic mass and a_0 is the Bohr radius) and a time step of $\delta t = 0.1$ fs to integrate the equations of motion. Temperature control is implemented for both ionic and electronic degrees of freedom by using Nosé-Hoover thermostats.^{27,28} We carried out simulations at $T=(1050\pm 10)$ K over a time periods of 40 ps, with statistical averages taken after discarding an initial segment of 2 ps. Since the use of the BLYP scheme is aimed at weakening the metallic character of bonding when compared to the PW one, it is worthwhile to check whether the comparison of the electronic densities of states for the PW and BLYP case substantiate this choice. As shown in Fig. 1, our selec-

tion of the exchange-correlation functional is legitimated by the comparison between the corresponding time averages (taken at the same temperature $T=(1050\pm 10)$ K) of the electronic densities of states. Indeed, the BLYP approach is seen to provide a deeper pseudo-gap around the Fermi level than the PW one.

III. REAL SPACE PROPERTIES

A. Pair correlation functions

Partial pair correlation functions $g_{\alpha\beta}(r)$ are shown in Fig. 2. Peak positions and number of neighbors within given integration ranges are displayed in Table I. Among the three pair correlation functions, $g_{\text{GeGe}}(r)$ is the one most affected by the choice of the exchange-correlation functional. The BLYP scheme improves upon the PW one by yielding a clear first maximum, due to homopolar Ge–Ge bonds, and a very pronounced first minimum, closely reproducing the trends observed in $g_{\text{GeGe}}^{\text{exp}}(r)$. In $g_{\text{GeGe}}^{\text{BLYP}}(r)$ the position of the first peak approaches the experimental value ($r = 2.45$ Å, BLYP; $r = 2.70$ Å, PW, Ref. 15 ; $r = 2.33$ Å, Ref. 6). Equally favorable is the BLYP prediction of the number of Ge in the first-neighbor shell (0.22, see Table I, to be compared with 0.25, Ref. 6) The shape of $g_{\text{GeGe}}^{\text{BLYP}}(r)$ reproduces the shoulder in the main peak occurring at $r\sim 3.1$ Å, indicative of edge sharing (ES) connections among tetrahedra.⁷ The Ge–Se pair correlation function $g_{\text{GeSe}}^{\text{exp}}(r)$ is characterized by a prominent main peak and a deep minimum. The position of the main peak is slightly displaced toward shorter distance, by 0.05 Å. The BLYP scheme is able to reproduce accurately the height of the first maximum and the abrupt decay from the first, sharp maximum down to vanishing values. The first shell of coordination has a number of neighbors (3.55) in very good agreement with experiments (3.50, see Table I). Little improvement is found for larger distances, both $g_{\text{GeSe}}^{\text{BLYP}}(r)$ and $g_{\text{GeSe}}^{\text{PW}}(r)$ lacking of the second, small maximum visible in $g_{\text{GeSe}}^{\text{exp}}(r)$. Both $g_{\text{SeSe}}^{\text{BLYP}}(r)$ and $g_{\text{SeSe}}^{\text{PW}}(r)$ follows closely the experimental $g_{\text{SeSe}}^{\text{exp}}(r)$ for $r > 3$ Å. The present set of calculations provides Se–Se correlations very similar to those obtained in Ref. 15, as shown by the close numbers for the first coordination shell neighbors (see Table I). Homopolar Se–Se bonds are found at a distance only 2% larger than in the PW case.

We obtain partial (n_{Ge} , n_{Se}) and average (n) coordination numbers from the first-neighbor coordination numbers, n_{GeGe} , n_{GeSe} , and n_{SeSe} , given in Table II. The resulting theoretical values are compared to experimental data in Table II. As pointed out in Ref. 15, a compensation occurred in the PW case between the underestimated value of n_{GeGe} and the overestimated value of n_{GeSe} , leading to a good agreement for n_{Ge} . In the present case, the small difference between n_{Ge} (BLYP) and its experimental counterpart is the result of close values for each single contributions, i.e. n_{GeGe} , n_{GeSe} ,

and n_{SeSe} . As a result, the calculated and experimental average coordination numbers n differ by only 3.5%.

Overall, the present calculations improve the short-range structure of l -GeSe₂, featuring more structured $g_{GeGe}^{exp}(r)$ and $g_{GeSe}^{exp}(r)$. In particular, the BLYP approach provides much shorter Ge–Ge distances and a well defined first shell of Ge neighbors, bringing pair correlation functions in better agreement with experiments.

B. Coordination numbers and bond angle distribution

Further insight into the network topology and its sensitivity to the specific exchange-correlation functional can be obtained through $n_\alpha(l)$. We define this quantity as the average number of atoms of species α l -fold coordinated (see Table III), where α are Ge or Se atoms. Consistently with the choice made in Ref. 15, we here used a cutoff distance of 3 Å, which corresponds to the first minimum in the Ge–Se pair correlation function and well describes the first shell of neighbors also for Ge–Ge and Se–Se correlations. As a first observation, one notices that the BLYP scheme is characterized by a higher proportion of Ge-GeSe₃ connections (as much as 23%), contributing to a percentage of Ge fourfold coordinated atoms moderately larger than in the PW case (66% against 61%). The increase of Ge–Ge homopolar bonds and Ge-GeSe₃ connections takes place at the expenses of the undefective GeSe₄ tetrahedra, lowering from 53.8% (PW) to 41.8% (BLYP). These data are a further manifestation of an increased number of Ge–Ge first-shell neighbors. The distribution of miscoordinated Ge atoms is different in the two situations: PW and BLYP favor threefold ($l=3$) and fivefold ($l=5$) connections, respectively. In particular, in Ge-GeSe₄ connections a homopolar Ge–Ge bond is found to coexist with an adjacent tetrahedral arrangement. Coordination of Se atoms reflects the increase of chemical order occurring within the BLYP scheme. The number of twofold coordinated Se atoms becomes more than 10% larger, mostly due to the predominant Se-Ge₂ configuration. A corresponding decrease in the number of miscorrelations (in particular Se-SeGe₂, lowering from 13% to 6.4% is noticeable in Table III).

In Fig. 3 we show the distribution of the Se–Ge–Se (θ_{SeGeSe}) and Ge–Se–Ge (θ_{GeSeGe}) bond angles. These distributions have been calculated by including neighbors separated by less than 3 Å. Two features are worth pointing out. First, the Se–Ge–Se bond angle distribution becomes highly symmetric around 109° in the BLYP description and has also a higher intensity. This stands for an improved tetrahedral order when compared to the results of Ref. 15, where the maximum occurred at 103° and the distribution has a larger width. Second, two distinct peaks are visible in the BLYP Ge–Se–Ge bond angle distribution at about 80° and 100° at the place of a flat maximum in between the same values. In Ref. 15 we showed that the Ge–Se–Ge bond angle distribution

can be decomposed in two contributions, one associated to edge-sharing tetrahedra (for values close to 80°) and the other due to corner-sharing tetrahedra (for values close to 100°). Similarly, the peaks visible in the shape of BLYP Ge–Se–Ge bond angle distribution have to be ascribed to these two different connections. Their prominent appearance stems from a improved tetrahedral organization, in line with the analysis of the coordination environment for Ge and Se.

Finally, we compare the number of Ge atoms that belong to zero, one, and two fourfold rings. We used the counting algorithm based on the shortest-path criterion first proposed by King and then improved by Franzblau.^{29,30,31} Cutoff radii were taken equal to 3.0 Å for Ge–Ge, Ge–Se and Se–Se interactions. By using the ring statistics results, Ge atoms can be termed Ge(0) (Ge atoms not belonging to any fourfold ring), Ge(1) (Ge atoms belonging to one fourfold ring), and Ge(2) (Ge atoms belonging to two fourfold rings). Ge(1) and Ge(2) form edge-sharing connections, while Ge(0) encompasses not only those Ge atoms involved in corner-sharing connections ($N_{Ge}(CS)$) but also some of the Ge atoms forming homopolar bonds, N_{Ge-Ge} . In Ref. 15 it was found that 55% of the Ge atoms do not belong to fourfold rings (Ge(0)), 36% belong to a single fourfold ring (Ge(1)), and 9% belong to two fourfold rings (Ge(2)). According to the present results obtained with the BLYP scheme 61% of the Ge atoms are Ge(0), 34% are Ge(1) and 5% are Ge(2). Therefore, Ge atoms involved in edge-sharing connections ($N_{Ge}(ES)$), according to PW and BLYP calculations, turn out to be $N_{Ge}(ES,PW)=45\%$ and $N_{Ge}(ES,BLYP)39\%$, respectively.

To obtain $N_{Ge}(CS)$, we adopted the proposal of Ref. 6, i.e. $N_{Ge}(CS)=1-N_{Ge}(ES)-N_{Ge-Ge}$, which holds in the absence of extended chains.⁶ By using the results of Table I ($N_{Ge-Ge}(BLYP)=22\%$, $N_{Ge-Ge}(PW)=4\%$) one obtains that $N_{Ge}(CS, PW)=51\%$ and $N_{Ge}(CS, BLYP)=39\%$, leading to $N_{Ge}(CS, PW)/N_{Ge}(ES, PW)=1.13$ and $N_{Ge}(CS, BLYP)/N_{Ge}(ES, BLYP)=1$ (these values are also collected in Table III). The full partial structure factor analysis of liquid GeSe₂ points toward comparable numbers for the edge-sharing and corner-sharing sites ($N_{Ge}(CS, BLYP)/N_{Ge}(ES, BLYP)\sim 1$).⁷ This is consistent with the experimental prediction of Ref. 7, where the number of edge-sharing and corner-sharing sites were found very close. Therefore, the BLYP approach proves more suitable to yield the correct relative proportion of corner-sharing and edge-sharing tetrahedra.

IV. RECIPROCAL SPACE PROPERTIES

A. Faber-Ziman and Bhatia-Thornton partial structure factors

In Fig. 4, we display the comparison between the two sets of calculated Faber-Ziman (FZ)³² partial structure factors (PW scheme, Ref. 15, and BLYP scheme, present

results) and their experimental counterpart.^{6,7} In Ref. 15 it was established that the performance of PW calculations were very satisfactory for k values characteristic of short range properties ($k > 2 \text{ \AA}^{-1}$). However, a major disagreement existed in the region of the FSDP (first sharp diffraction peak), at $k \sim 1. \text{ \AA}^{-1}$, in particular for the $S_{GeGe}^{PW}(k)$ structure factor and, to a lesser extent, for the $S_{GeSe}^{PW}(k)$ structure factor. Moreover, $S_{GeGe}^{PW}(k)$ was found to be less structured and slightly shifted towards smaller wavevectors with respect to the experimental curve. For $k > 1.5 \text{ \AA}^{-1}$ a clear improvement is noticeable in the shape of $S_{GeGe}(k)$ around the second maximum, that superposes to the experimental result, the peak position being located at 2.2 \AA^{-1} (PW calculations, 1.88 \AA^{-1} , experimental value, 2.2 \AA^{-1} .^{7,15}) The position of the FSDP in $S_{GeGe}(k)$ is shifted leftward improving upon the result of Ref. 15 in both location and height. However, a second spurious peak in the FSDP region shows up at larger k values, suggesting that our statistical accuracy might be further improved by longer runs and/or larger simulation cells. In the case of $S_{GeSe}(k)$, the FSDP height is reduced and the shape of the first minimum follows closely the experimental profile, bringing theory in better agreement with the experimental result. As to $S_{SeSe}(k)$, both the present approach and the one of Ref. 15 performs very well over the entire range of k values. These pieces of evidence confirm that BLYP concur to improve the short-range behavior pertaining to Ge atoms, while the changes induces in the intermediate range behavior are smaller.

In this context, it is worthwhile to analyze the comparison between theory and experiments by considering the Bhatia-Thornton³³ partial structure factors $S_{NN}(k)$ (number-number), $S_{NC}(k)$ (number-concentration) and $S_{CC}(k)$ (concentration-concentration) (see Fig. 5) These can be obtained by linear combinations of the FZ structure factors.³² In terms of the Bhatia-Thornton structure factors, the total neutron structure factor $S_T(k)$ reads:

$$S_T(k) = S_{NN}(k) + A[S_{CC}(k)/c_{Ge} c_{Se} - 1] + B S_{NC}(k), \quad (1)$$

where $A = c_{Ge}c_{Se}\Delta b^2/\langle b \rangle^2$, $B = 2\Delta b/\langle b \rangle$, $\Delta b = b_{Ge} - b_{Se}$, $\langle b \rangle = c_{Ge}b_{Ge} + c_{Se}b_{Se}$, c_α and b_α denoting the atomic fraction and the coherent scattering length of the chemical species α ($b_{Ge}=8.185 \text{ fm}$, $b_{Se}=7.97 \text{ fm}$)⁷. This leads to coefficients A and B equal to 1.6×10^{-4} and 0.053 , respectively. As detailed in Ref. 15, $S_{NN}(k)$ is a very good approximation for the total neutron structure factor $S_T(k)$, i.e. $|S_T(k) - S_{NN}(k)| < 0.015$.

As shown in Fig. 5, both $S_{NN}^{PW}(k)$ and $S_{NN}^{BLYP}(k)$ are in excellent agreement with experiments, following closely the experimental data over the entire range of k values. BLYP improves upon PW in the position of the FSDP, that is closer to the measured value (0.98 \AA^{-1} , Ref. 7, 1.01 \AA^{-1} , present results, 1.13 \AA^{-1} , Ref. 15) and better reproduces the experimental data in the range $2 \text{ \AA}^{-1} < k < 4 \text{ \AA}^{-1}$. Similar performances are also recorded for the case of $S_{NC}(k)$. Most interesting

is the case of the concentration-concentration structure factor $S_{CC}^{exp}(k)$ in the region $k < 2. \text{ \AA}^{-1}$. In recent years, the occurrence of the FSDP in the concentration-concentration structure factor $S_{CC}^{exp}(k)$ has stimulated intense experimental and theoretical work, in the search of its microscopic origins.^{34,35,36,37} With this purpose in mind, the intensities of the FSDP in the $S_{CC}(k)$ have been compared for a series of liquid and glasses.²² It was showed that the FSDP in $S_{CC}(k)$ occurs for moderate departures from chemical order, but vanishes either when the chemical order is essentially perfect or for high levels of structural disorder. This is exactly the case of liquid GeSe_2 modeled within the PW scheme, for which no FSDP appear in the $S_{CC}(k)$.^{13,15} Given these premises, the question arises on whether the higher tetrahedral order exhibited by the present model of liquid GeSe_2 scheme does result in any improvement in the behavior of the FSDP in $S_{CC}(k)$. Although a small shoulder has appeared at the FSDP location in $S_{CC}^{BLYP}(k)$, the prominent experimental peak remains largely underestimated. The results on the partial structure factor support the notion that the use of the BLYP generalized gradient approximation has a much larger effect on to the short-range properties than on the intermediate-range ones.

V. DYNAMICAL PROPERTIES

Diffusion coefficients are sensitive probes of the structural organization in disordered network-forming materials. On the one hand, in a chemically ordered network, the tetrahedra are the main constitutive units, their stability strongly reducing atomic mobility. On the other hand, departures from chemical order (homopolar bonds, miscoordinations) favor atomic mobility since the network can seek the energetically most favorable arrangements through bond coordination changes. In a recent paper, we have provided a revealing example of the correlation existing between the values of the diffusion coefficients and the network structure.³⁸ In Ref. 38 we have compared structural and dynamical properties of liquid GeSe_2 as obtained from FPMD and an effective potentials based the polarizable ionic model (PIM). While a sizeable departure from chemical order is found in the FPMD model, the PIM structure is highly chemically ordered and the GeSe_4 tetrahedron is largely predominant among the structural units. As a consequence of these drastic structural differences, the diffusion coefficients pertaining to the PIM model are as low as $\sim 1 \times 10^{-6} \text{ cm}^2 \text{ s}^{-1}$ at $T=3000 \text{ K}$, while they are at least ten times larger in the FPMD case at $T=1050 \text{ K}$ (see below). Having established that the tetrahedral order is larger in the BLYP model than in the PW one for $l\text{-GeSe}_2$ at $T=1050 \text{ K}$, it is of interest to see to what extent this is reflected in the values of the corresponding diffusion coefficients.

The comparison between the calculated statistical average of the mean square displacement

$$\langle r^2(t) \rangle = \frac{1}{N_\alpha} \left\langle \sum_{i=1}^{N_\alpha} |\mathbf{r}_{i\alpha}(t) - \mathbf{r}_{i\alpha}(0)|^2 \right\rangle \quad (2)$$

for both species α , Ge and Se, obtained within the PW (Ref.) and the BLYP schemes, is shown in Fig. 6. In Eq. (2), $\mathbf{r}_{i\alpha}(t)$ is the coordinate of the i th particle at time t and N_α is the number of particles of the species α . The diffusive regime is associated with a slope equal to 1 in the infinite time limit linear behavior of $\log \langle r^2(t) \rangle$ vs $\log t$. Provided this condition holds, the diffusion constant can be obtained as

$$D = \frac{\langle r^2(t) \rangle}{6t} \quad (3)$$

In Ref. 15, asymptotic values of $\langle r^2(t) \rangle$ are attained after 5–6 ps to give diffusion coefficients of $D_{Ge} = (2.2 \pm 0.2) \times 10^{-5} \text{ cm}^2/\text{s}$ and $D_{Se} = (2.2 \pm 0.2) \times 10^{-5} \text{ cm}^2/\text{s}$. In the present case, establishment of a diffusive regime requires longer time intervals and asymptotic values of $\langle r^2(t) \rangle$ could only be extrapolated in Fig. 6. The estimated diffusion coefficient takes the value of $D_\alpha = (0.2 \pm 0.2) \times 10^{-5} \text{ cm}^2/\text{s}$ for both $\alpha = \text{Ge}$ and Se . To allow a comparison with experimental data, we use the Eyring relationship;

$$D = \frac{kT}{\eta\lambda} \quad (4)$$

where λ is a typical hopping length for the diffusing atom³⁹ and η is the viscosity. In silicate melts such as Na_2SiO_3 , Eq. (4) holds satisfactorily with $\lambda = 2.8 \text{ \AA}$, a distance typical of Si-Si and O-O separation in these melts.⁴⁰ By exploiting viscosity data of liquid GeSe_2 , together with a choice of λ close to the Ge-Ge and Se-Se separation distances (3.7 \AA), we obtain for the temperatures $T = 1050 \text{ K}$ a diffusion coefficient $D_{\alpha,exp} = 0.045 \times 10^{-5} \text{ cm}^2 \text{ s}^{-1}/\text{s}$.⁴¹ This estimate can be taken as a lower bound in Eq. (4), since the account of homopolar bonds for both species increases λ . The present calculations are in better agreement with the estimated value of D_α than the results of Ref. 15. Such improved agreement is consistent with the partially restored tetrahedral order that characterizes our real space data. Restored tetrahedral order enhances the strength of the network, thereby reducing the atomic mobility.

VI. DISCUSSION

In view of the above pieces of evidence, it appears that the structure of a prototypical network-forming material, such as $l\text{-GeSe}_2$, is highly sensitive to the specific exchange-correlation functionals employed with DFT. In particular, the extent of the departure from perfect chemical order (i.e. no homopolar bonds and all Ge atoms

four-fold coordinated) depends on the spatial distribution of the valence charge density. In the case of moderate difference of electronegativity between the component systems, the account of the delicate balance between electron localization on the atomic sites (i.e. ionic bonding) and electronic delocalization (i.e. covalent effects and/or tendency toward metallic bonding) becomes a challenging issue for atomic-scale modelling. Liquid GeSe_2 proved to be an interesting benchmark systems for theoretical approaches, due to the concomitant presence of close percentages of corner- and edge-sharing connections, homopolar bonds and fluctuations of concentrations on intermediate range distances. Early effective potentials based on the coulombic interactions between formal charges provide the extreme case of ionic interactions, leading to networks made of undefective tetrahedra and the absence of homopolar bonds.⁸ The inclusion of polarization effects and/or many body forces allows for the presence of edge-sharing tetrahedra, in agreement with experimental results.^{8,9,10,38} The use of DFT models proved necessary to obtain defective tetrahedra (Ge atoms not fourfold coordinated) and homopolar bonds for both Se and Ge atoms, as found in the experiments. However, the mere application of a fully self-consistent LDA had the effect of overestimating the chemical disorder. This has led to the lack of intermediate range order and to an overall atomic structure in worse agreement with the experiment than that obtained with interatomic potentials.¹⁴ These shortcomings were traced back to an insufficient treatment of the ionicity, i.e. an insufficient valence charge localization on the atomic sites, strongly affecting the stability of GeSe_4 tetrahedra. To go beyond these limitations of the LDA-DFT approach, we have applied the generalized gradient approximation of DFT in two subsequent steps. In the first (Ref. 14) a functional rooted on the electron gas model has allowed to recover a very good agreement with the experiments in terms of structural properties. In the second (this work) a further refinement aimed at a more enhanced valence charge localization on the atomic site has improved the short range properties, in particular those related to the Ge close environment.

It is useful in this context to recall the role played by specific structural features in determining a realistic network structure. The following ideas apply to the whole family of A_nX_{1-n} ($\text{A} = \text{Ge}, \text{Si}; \text{X} = \text{O}, \text{S}, \text{Se}$) disordered systems. The structural features we refer to are : *a*) homopolar bonds and miscoordinations and *b*) edge-sharing tetrahedra vs corner-sharing tetrahedra. Being able to correctly describe the departure from chemical order (occurring because of miscoordinations and homopolar bonds) is crucial for two reasons. First, it allows to model the short range structure reliably improving upon simplified models consisting of perfect tetrahedra connected to each other. Second, it has a profound impact on the intermediate range properties, which were found to be strongly dependent on the existence of a moderate amount of chemical disorder. As detailed in a previous

paper, no intermediate range order exist either in perfect tetrahedral or in highly disordered networks.²² The establishment of the intermediate range order is also very much sensitive to the occurrence of edge-sharing tetrahedra. Recently, it has been shown that the first sharp diffraction peak in the concentration-concentration structure factor $S_{CC}(k)$ is due to chains of edge-sharing tetrahedra.³⁶ This result correlates a specific structural subunit to the intermediate range order, exemplifying how an accurate description allows to link microscopic features to measurable properties.

VII. CONCLUSION

We have studied the short and intermediate range properties of liquid GeSe₂ at T=1050 K in the framework of first-principle molecular dynamics by using for the generalized gradient approximation the BLYP scheme. Our motivation rests on the outcome of a previous investigation, carried out within the same theoretical framework but employing a different recipe (the one due to Perdew and Wang, PW) for the generalized gradient approximation.¹⁵ In that work, it was stressed that the comparison between theory and experiment was excellent at the level of the total neutron structure factor, but less satisfactory in terms of the partial correlations both in real and reciprocal space. We recall that in Ref. 15, the Ge–Ge pair correlation function was less structured

than the experimental counterpart, the first neighbors distances exceeded the experimental values by about 15 % and no features were found at the FSDP location in the concentration-concentration structure factor. The use of the BLYP exchange-correlation functional substantially improves the short-range properties of liquid GeSe₂. The shapes of the Ge–Ge and (to a lesser extent) the Ge–Se pair correlation functional are more structured and are consistent with a higher level of tetrahedral organization, i.e. the network is less affected by coordinations other than the fourfold one (GeSe₄ tetrahedra). The same occurs for the Se–Ge–Se and Ge–Se–Ge bond angle distributions, the first more symmetric around the tetrahedral angle 109° while the second shows two distinct peaks accounting for edge-sharing and corner-sharing connections. Higher tetrahedral order results in lower diffusion coefficient for both species. The impact of the BLYP scheme on the intermediate range properties is more elusive. Smaller improvements are found for the intensity and the position of the peaks located at low k values in the partial structure factor. Work is in progress to investigate the impact of hybrid exchange-correlation functionals on the network properties of disordered chalcogenides.⁴²

VIII. ACKNOWLEDGEMENT

We thank P. S. Salmon and M. Boero for stimulating exchanges.

-
- ¹ P. Tronc, M. Bensoussan, A. Brenac and C. Sebenne, *Phys. Rev. B* **8**, 5947 (1973).
² R. Azoulay, H. Thibierge and A. Brenac, *J. Non-Cryst. Solids* **18**, 33 (1975).
³ P. S. Salmon and J. Liu, *J. Phys. Condens. Matter* **6**, 1449 (1994).
⁴ P. Boolchand and W.J. Bresser, *Phil. Mag. B* **80**, 1757 (2000).
⁵ C. Massobrio, F.H.M. van Roon, A. Pasquarello, and S. W. De Leeuw, *J. Phys.: Condens. Matter* **12**, L697, (2000).
⁶ I. Petri and P. S. Salmon, *J. Phys. Condens. Matter* **15**, S1509 (2003).
⁷ I.T. Penfold and P.S. Salmon, *Phys. Rev. Lett.* **67**, 97 (1991).
⁸ P. Vashishta, R.K. Kalia and I. Ebbsjö, *Phys. Rev. B* **39**, 6034 (1989).
⁹ J.C. Mauro and A.K. Varshneya, *J. Am. Ceram. Soc.* **89**, 2323 (2006).
¹⁰ J.C. Mauro and A.K. Varshneya, *J. Am. Ceram. Soc.* **90**, 192 (2007).
¹¹ M. Cobb, D.A. Drabold and R.L. Cappelletti, *Phys. Rev. B* **54**, 12162 (1996).
¹² M. Cobb and D.A. Drabold, *Phys. Rev. B* **56**, 3054 (1997).
¹³ C. Massobrio, A. Pasquarello, and R. Car, *Phys. Rev. Lett.* **80**, 2342 (1998).
¹⁴ C. Massobrio, A. Pasquarello, and R. Car, *J. Am. Chem. Soc.* **121**, 2943 (1999).
¹⁵ C. Massobrio, A. Pasquarello, and R. Car, *Phys. Rev. B* **64**, 144205 (2001).
¹⁶ C. Massobrio and A. Pasquarello, *Phys. Rev. B* **77**, 144207 (2008).
¹⁷ J. P. Perdew and Y. Wang, *Phys. Rev. B* **45**, 13244 (1992).
¹⁸ A. D. Becke, *Phys. Rev. A* **38**, 3098 (1988).
¹⁹ C. Lee, W. Yang and R.G. Parr, *Phys. Rev. B* **37**, 785 (1988).
²⁰ B. G. Johnson, P.M.W. Gill and J.A. Pople, *J. Chem. Phys.* **98**, 5612 (1993).
²¹ R. Colle and D. Salvetti, *Theor. Chim. Acta* **37**, 329 (1975).
²² C. Massobrio, M. Celino, and A. Pasquarello, *Phys. Rev. B* **70**, 174202 (2004).
²³ R. Car and M. Parrinello, *Phys. Rev. Lett.* **55**, 2471 (1985).
²⁴ J. Sarnthein, A. Pasquarello and R. Car, *Phys. Rev. Lett.* **74**, 4682 (1995); *Phys. Rev. B* **52**, 12690 (1995).
²⁵ N. Trouiller and J.L. Martins, *Phys. Rev. B* **43**, 1993 (1991).
²⁶ K. P. Huber and G. Herzberg, *Molecular Spectra and Molecular Structure, IV. Constants of Diatomic Molecules* (Van Nostrand, Princeton, 1979).
²⁷ S. Nosé, *Mol. Phys.* **52**, 255 (1984); W. G. Hoover, *Phys. Rev. A* **31**, 1695 (1985).
²⁸ P.E. Blöchl and M. Parrinello, *Phys. Rev. B* **45**, 9413 (1992).
²⁹ S.V. King, *Nature* **213**, 1112 (1967).
³⁰ D.S. Franzblau, *Phys. Rev. B* **44**, 4925 (1991).
³¹ V. Rosato, M. Celino, G. Benedek, and S. Gaito, *Phys.*

- Rev. B **60**, 16928 (1999).
- ³² The relationship between the three sets of partial structure factors commonly used (Faber-Ziman, Ashcroft-Langreth and Bhatia-Thornton) can be found in Y. Waseda, *The Structure of Non-Crystalline Materials*, (McGraw-Hill, New York, 1980).
- ³³ A. Bhatia and D. Thornton, Phys. Rev. B **2**, 3004 (1970).
- ³⁴ P.S. Salmon, Proc. R. Soc. London A **437**, 591 (1992).
- ³⁵ C. Massobrio and A. Pasquarello, J. Chem. Phys. **114**, 7976 (2001).
- ³⁶ C. Massobrio and A. Pasquarello, Phys. Rev. B **75**, 014206 (2007).
- ³⁷ B.K. Sharma and M. Wilson, Phys. Rev. B **73**, 060201(R) (2006).
- ³⁸ M. Wilson, B.K. Sharma and C. Massobrio, J. Chem. Phys. **128**, 244505 (2008).
- ³⁹ S. Glasstone, K.J. Laidler and H. Eyring, *The Theory of Rate Processes*, (McGraw-Hill, New York, 1941).
- ⁴⁰ B.O. Mysen and P. Richet, *Silicate Glasses and Melts: Structure and Properties*, (Springer, Berlin, 2005).
- ⁴¹ S. Stølen, T. Grande and H.-B. Johnsen, Phys. Chem. Chem. Phys. **4**, 3396 (2002).
- ⁴² A. D. Becke, J. Chem. Phys. **98**, 5648 (1993).

TABLE I: First (FPP) and second (SPP) peak positions in experimental (Ref. 6,7) and theoretical $g_{\alpha\beta}(r)$. BLYP: present calculations, PW: calculation of Ref. 15. The integration ranges corresponding to the coordination numbers $n_{\alpha\beta}$ and $n'_{\alpha\beta}$ are 0–2.6 Å, 2.6–4.2 Å for $g_{GeGe}(r)$, 0–3.1 Å, 3.1–4.5 Å for $g_{GeSe}(r)$ and 0–2.7 Å, 2.7–4.8 Å for $g_{SeSe}(r)$. Error bars are the standard deviations from the mean for subaverages of 2 ps.

$g_{\alpha\beta}(r)$	FPP (Å)	$n_{\alpha\beta}$	SPP (Å)	$n'_{\alpha\beta}$
$g_{GeGe}^{BLYP}(r)$	2.45±0.10	0.22±0.01	3.67±0.10	2.70±0.06
$g_{GeGe}^{PW}(r)$	2.70±0.10	0.04±0.01	3.74±0.05	2.74±0.06
$g_{GeGe}^{exp}(r)$	2.33±0.03	0.25±0.10	3.59±0.02	2.9±0.3
$g_{GeSe}^{BLYP}(r)$	2.36±0.10	3.55±0.01	5.67±0.02	3.85±0.06
$g_{GeSe}^{PW}(r)$	2.41±0.10	3.76±0.01	5.60±0.01	3.72±0.03
$g_{GeSe}^{exp}(r)$	2.42±0.02	3.5±0.2	4.15±0.10	4.0±0.3
$g_{SeSe}^{BLYP}(r)$	2.38±0.02	0.33±0.01	3.83±0.02	8.9±0.06
$g_{SeSe}^{PW}(r)$	2.34±0.02	0.37±0.01	3.84±0.02	9.28±0.04
$g_{SeSe}^{exp}(r)$	2.30±0.02	0.23±0.05	3.75±0.02	9.6±0.3

TABLE II: Experimental and theoretical values for the partial coordination numbers n_{Ge} and n_{Se} and the average coordination number n of liquid GeSe₂ at T=1040 K. BLYP: present calculations, PW: calculation of Ref. 15. The coordination numbers n_{Ge} and n_{Se} are given by $n_{GeGe} + n_{GeSe}$ and $n_{SeSe} + n_{SeGe}$, respectively (see the values reported in Table I for n_{GeGe} , n_{GeSe} and n_{SeSe} , where $n_{GeSe} = 2n_{SeGe}$). The average coordination number n is equal to $c_{Ge}(n_{GeGe} + n_{GeSe}) + c_{Se}(n_{SeSe} + n_{SeGe})$. The experimental values extracted from Ref. 6 are also reported. Error bars are the standard deviations of the mean for subaverages of 2 ps.

	n_{Ge}	n_{Se}	n
BLYP	3.77±0.02	2.11±0.02	2.66±0.02
PW	3.80±0.02	2.25±0.02	2.77±0.02
Ref. 6	3.75±0.3	1.98±0.15	2.57±0.20

TABLE III: Average number $n_\alpha(l)$ (expressed as a percentage) of Ge and Se atoms l -fold coordinated at a distance of 3.0 Å. For each value of $n_\alpha(l)$, we give the identity and the number of the Ge and Se neighbors. For instance, GeSe₃ with $l=4$ means a fourfold coordinated Ge with one Ge and three Se nearest-neighbors. Values smaller than 1 are reported only for sake of comparison with corresponding values equal or larger than 1. In parenthesis: results of Ref. 15. We also compare calculated and experimental values (in percentage) for the number of Ge atoms forming edge-sharing connections, $N_{\text{Ge}}(\text{ES})$, the number of Ge atoms forming corner-sharing connections, $N_{\text{Ge}}(\text{CS})$ and the number of Ge atoms involved in homopolar bonds, $N_{\text{Ge-Ge}}$. Experimental values are taken from Ref. 6.

Ge	$l = 2$		$l = 3$	
	Se ₂	4.0 (5.2)	GeSe ₂	0.8 (2.6)
			Se ₃	13.5 (19.8)
	$l = 4$		$l = 5$	
	GeSe ₃	23.3 (7.0)	Ge ₂ Se ₃	2.4 (0.4)
	Se ₄	41.8 (53.8)	GeSe ₄	11.7 (5.9)
		Se ₅	0.6 (4.6)	
Se	$l = 1$		$l = 2$	
	Ge	0.9 (1.7)	Se ₂	3.6 (2.8)
			SeGe	20.7 (21.9)
			Ge ₂	59.2 (45.6)
	$l = 3$		$l = 4$	
	Se ₂ Ge	2.4 (3.2)	SeGe ₃	0.3 (1.0)
SeGe ₂	5.8 (8.6)			
Ge ₃	6.4 (13.1)			
	$N_{\text{Ge}}(\text{ES})$	$N_{\text{Ge}}(\text{CS})$	$N_{\text{Ge-Ge}}$	
This work	39	39	22	
Ref. 15	45	51	4	

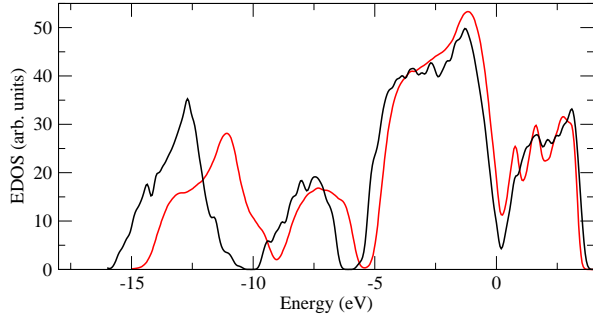


FIG. 1: (color on line) Electronic density of states (Kohn-Sham eigenvalues) of liquid GeSe_2 : black line: present BLYP results, red line: PW results of Ref. 15. A gaussian broadening of 0.1 eV has been employed.

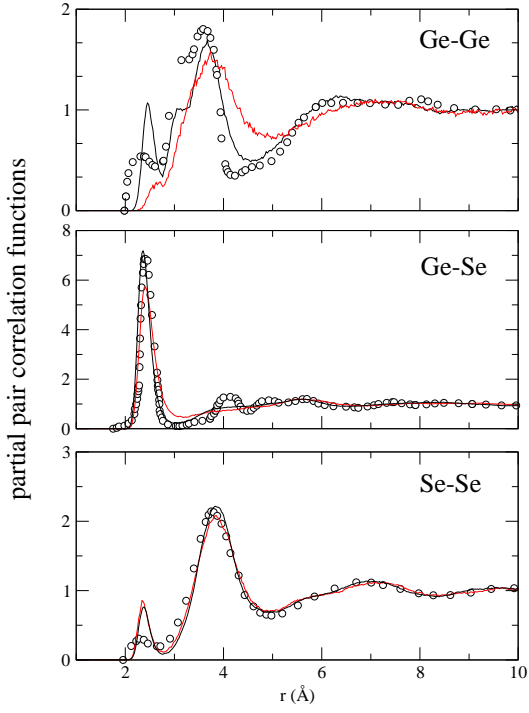


FIG. 2: (color on line) Partial pair correlation functions for liquid GeSe_2 : black line: present BLYP results, red line: PW results of Ref. 15, open circles: experimental results of Ref. 7.

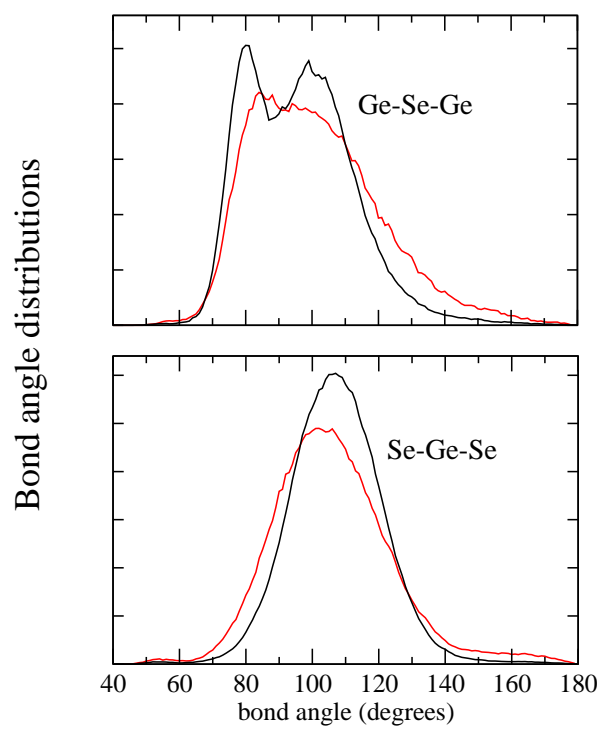


FIG. 3: (color on line) Bond-angle distributions Ge–Se–Ge (top) and Se–Ge–Se (bottom). black line: present BLYP results, red line: PW results of Ref. 15.

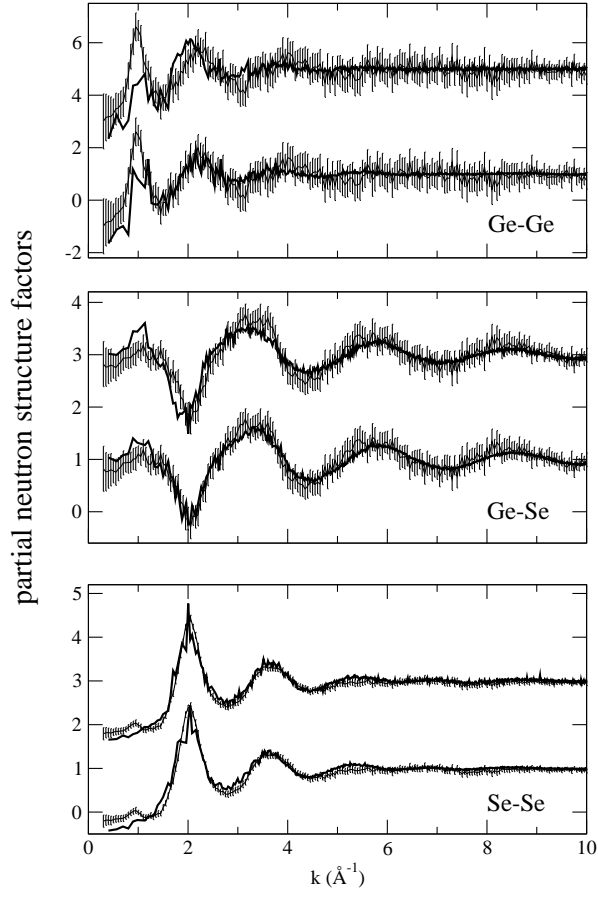


FIG. 4: Faber-Ziman partial structure factors for liquid GeSe_2 . In each panel, the experimental results of Ref. 7 are compared with the present BLYP results (bottom part) and with the PW results of Ref. 15 (top part). $S_{\text{GeGe}}^{PW}(k)$, $S_{\text{GeSe}}^{PW}(k)$ and $S_{\text{SeSe}}^{PW}(k)$ have been shifted up by 4, 2, and 2, respectively.

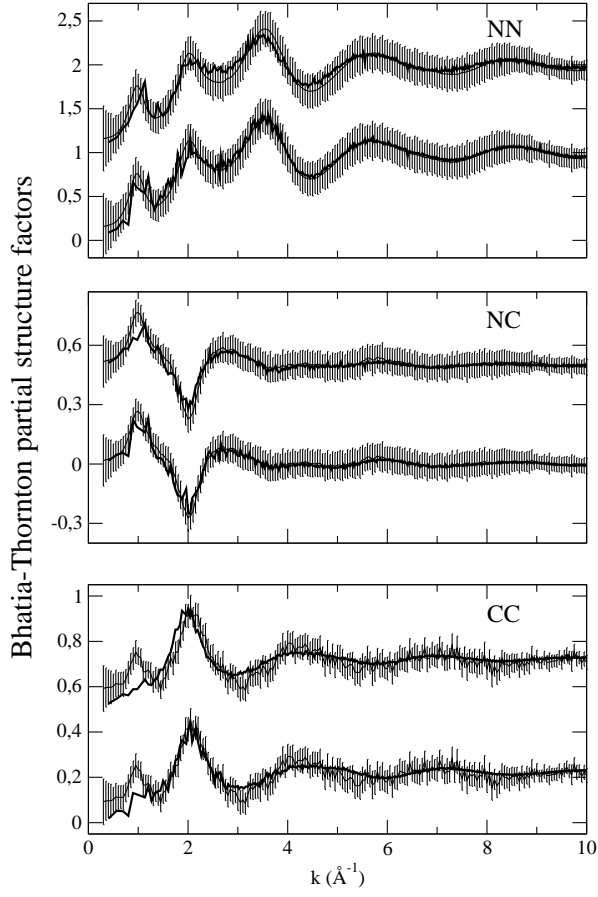


FIG. 5: Bhatia-Thornton partial structure factors for liquid GeSe_2 . In each panel, the experimental results of Ref. 7 are compared with the present BLYP calculations (bottom part) and with the PW calculations of Ref. 15 (top part). $S_{NN}^{PW}(k)$, $S_{NC}^{PW}(k)$ and $S_{CC}^{PW}(k)$ have been shifted up by 1, 0.6, and 0.5, respectively.

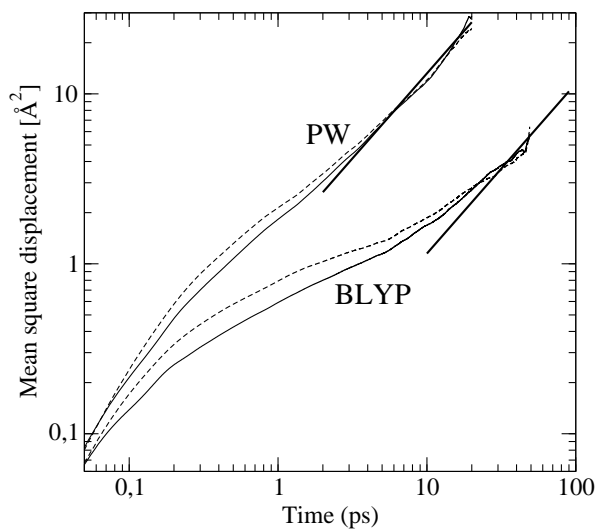


FIG. 6: Average mean square displacements for Ge (dashed line) and Se atoms (full line) of liquid GeSe_2 . The infinite time behavior corresponding to a slope equal to 1 in the $\log\text{-}\log$ plot of $\langle r^2(t) \rangle$ vs t is also shown.